appears to be consistent, i.e., $-\Delta H$ for P-I > P-I-18C6 > P18C6 for both picrate and methyl orange.

It is not easy to rationalize the strong exothermicity of picrate binding to P-I. Hydrophobic interactions of organic solutes with macromolecules generally have low ΔH and frequently positive ΔS values, as in the binding of methyl orange to P18C6[1] or other polymers. As implied by the optical shift, picrate anions, on binding to P-I, release hydration water, and this is expected to increase the entropy of binding, but other factors may be more important. For example, cation binding to a cryptand ligand also releases hydration water, but the process for Rb^+ or Cs^+ in water is accompanied by a decrease in entropy of as much as −20 eu.[28] It may be that on binding picrate to the tightly coiled P-I molecule the expansion of the chain needed to accommodate the large anion may permit some water to penetrate into the polymer domain and to hydrogen bond to the glyme oxygen atoms. This at least could be one possible cause for the large negative ΔH and ΔS values, but more work is required to verify this.

In conclusion, it was shown that in aqueous solution some of the poly(vinylbenzoglymes) assume tightly coiled conformations and exhibit micellar character with strong binding of organic solutes such as picrate anions or methyl orange. Binding of alkali ions to these neutral polymers is very weak in water, but incorporation of crown ether monomers into these polymers provides a means to convert the poly(vinylbenzoglymes) into positively charged species using crown ether complexable cations. This further promotes and regulates the binding of organic anions. Extraction data show that in a solvent such as methylene chloride cation binding to the poly(vinylbenzoglymes) can be considerably more effective than to the corresponding monomeric analogues due to cooperative interactions with oxygen atoms of neighboring glyme chains which provides a more complete solvation shell for the cations.

Acknowledgment. The authors gratefully acknowledge the financial support of the National Science Foundation through Grant No. CHE 7905890.

References and Notes

(1) L. Wong and J. Smid, *J. Am. Chem. Soc.*, **99**, 5637 (1977).
(2) J. Smid, S. C. Shah, R. Sinta, A. J. Varma, and L. Wong, *Pure Appl. Chem.*, **51**, 111 (1979).
(3) S. C. Shah and J. Smid, *J. Am. Chem. Soc.*, **100**, 1426 (1978).
(4) L. Wong and J. Smid, *Polymer*, in press.
(5) L. D. Taylor and L. D. Cerankowski, *J. Polym. Sci., Polym. Chem. Ed.*, **13**, 2551 (1975).
(6) J. Smid, B. ElHaj, T. Majewicz, A. Nonni, and R. Sinta, *Org. Prep. Proced. Int.*, **8**, 193 (1976).
(7) S. Shah, S. Kopolow, and J. Smid, *Polymer*, in press.
(8) H. K. Frensdorff, *J. Am. Chem. Soc.*, **93**, 4684 (1971).
(9) S. Kopolow, T. E. Hogen Esch, and J. Smid, *Macromolecules*, **6**, 133 (1973).
(10) K. H. Wong, K. Yagi, and J. Smid, *J. Membr. Biol.*, **18**, 379 (1974).
(11) H. K. Frensdorff, *J. Am. Chem. Soc.*, **93**, 600 (1971).
(12) F. Vögtle and E. Weber, *Kontakte*, **1**, 11 (1977).
(13) B. Tümmler, G. Maass, E. Weber, W. Wehner, and F. Vögtle, *J. Am. Chem. Soc.*, **99**, 4683, (1977).
(14) L. L. Chan, K. H. Wong, and J. Smid, *J. Am. Chem. Soc.*, **92**, 1955 (1970).
(15) U. Takaki and J. Smid, *J. Am. Chem. Soc.*, **96**, 2588 (1974).
(16) J. Smid and A. M. Grotens, *J. Phys. Chem.*, **77**, 2377 (1973).
(17) J. J. Mooy, A. A. K. Klaassen, E. de Boer, H. M. L. Degens, Th. E. M. vanden Hark, and J. H. Noordik, *J. Am. Chem. Soc.*, **98**, 680 (1976).
(18) J. J. Mooy, A. A. K. Klaassen, and E. de Boer, *Mol. Phys.*, **32**, 879 (1976).
(19) M. Shinohara, J. Smid, and M. Szwarc, *J. Am. Chem. Soc.*, **90**, 2175 (1968).
(20) G. Chaput, G. Jeminet, and J. Juillard, *Can. J. Chem.*, **53**, 2240 (1975).
(21) K. H. Wong, G. Konizer, and J. Smid, *J. Am. Chem. Soc.*, **92**, 666 (1970).
(22) C. Tanford, "Physical Chemistry of Macromolecules", Wiley, New York, 1961.
(23) H. Schott, *J. Colloid Interface Sci.*, **24**, 193 (1967).
(24) I. M. Klotz, F. M. Walker, and R. B. Pivan, *J. Am. Chem. Soc.*, **68**, 1486 (1946).
(25) I. M. Klotz and K. Shikama, *Arch. Biochem. Biophys.*, **123**, 551 (1968).
(26) K. Kobayashi and H. Sumitomo, private communication. We thank these authors for communicating their data to us prior to publication.
(27) F. Cramer, W. Saenger, and H. Ch. Spath, *J. Am. Chem. Soc.*, **89**, 14 (1967).
(28) E. Kauffmann, J. M. Lehn, and J. P. Sauvage, *Helv. Chim. Acta*, **59**, 1099 (1976).

Dimensional and Hydrodynamic Properties of Poly(hexyl isocyanate) in Hexane

Hirochika Murakami, Takashi Norisuye,* and Hiroshi Fujita

Department of Polymer Science, Osaka University, Toyonaka, Osaka, 560 Japan.
Received November 6, 1979

ABSTRACT: Narrow-distribution fractions of poly(hexyl isocyanate) (PHIC) ranging in weight-average molecular weight $\bar{M}_w$ from 7×10^4 to 7×10^6 were studied by light scattering, viscosity, and sedimentation velocity measurements with hexane of 25 °C as a solvent. The molecular-weight dependence of the z-average mean-square radius of gyration $\langle S^2 \rangle_z$ was analyzed in terms of the Benoit–Doty theory for the Kratky–Porod wormlike chain, with the result that the persistence length q is 42 ± 1 nm and the molar mass per unit contour length M_L is 715 ± 15 nm^{-1}. With these parameter values, the measured values of $\langle S^2 \rangle_z$ as well as the angular dependence of the particle scattering function can be accurately fitted to the known theories for the wormlike chain model. When the data for the intrinsic viscosity $[\eta]$ and the sedimentation coefficient s_0 were compared with those of Yamakawa–Fujii's theories for the wormlike cylinder, with q and M_L fixed to 42 nm and 715 nm^{-1}, respectively, it was found that the best agreement between theory and experiment can be obtained only if inconsistent values, 1.6 nm for $[\eta]$ and 2.5 nm for s_0, are used for the diameter of the cylinder.

The recent calculations by Yamakawa and Fujii[1,2] of the intrinsic viscosity $[\eta]$ and sedimentation coefficient s_0 of a wormlike cylinder have afforded methods for estimating the parameters q, M_L, and d from viscosity and sedimentation velocity measurements. Here q, M_L, and d represent, respectively, the persistence length, the molar mass per unit contour length, and the diameter of the cylinder. However, the validity of these methods was suspected

0024-9297/80/2213-0345$01.00/0

when Godfrey and Eisenberg[3] applied them to carefully determied data of $[\eta]$ and s_0 for DNA, with the result that the d value estimated from $[\eta]$ was about one-half that from s_0. The DNA is a typical stiff chain polymer and may well be represented by a wormlike cylinder. Thus the result of Godfrey and Eisenberg may go into a critisism of the physical approximations adopted in formulating Yamakawa–Fujii's theories[1,2] of polymer hydrodynamics. The present paper describes a test of Yamakawa–Fujii's theories with poly(hexyl isocyanate) (PHIC), another well-known example of a stiff polymer.

Schneider et al.[4] were the first to investigate PHIC in dilute solution by light scattering and viscometry. Their study revealed an unmistakable stiffness of this polymer. The subsequent investigations by Berger and Tidswell[5] and also by Rubingh and Yu[6] showed that the PHIC chain in tetrahydrofuran and in hexane can be represented by the wormlike chain model. However, the data of these two groups are insufficient for an accurate check of existing theories of wormlike chains to be made. The molecular weights of the PHIC fractions studied by Berger and Tidswell cover only one decade from 4×10^4 to 4×10^5, and the experiment of Rubingh and Yu, though covering a much broader range of molecular weight, gives only a limited number of data points, seven for $\langle S^2 \rangle$ and six for $[\eta]$. Here $\langle S^2 \rangle$ is the mean-square radius of gyration of a polymer. It is to be noted that no sedimentation velocity data on PHIC have yet been reported. In the study described below, with hexane of 25 °C chosen as a solvent as in the work of Rubingh and Yu,[6] 19 well-fractionated samples of PHIC ranging in molecular weight from 7×10^4 to 7×10^6 were examined by light scattering, viscometry, and ultracentrifugation.

Experimental Section

Samples. Three PHIC samples, JH-1 ($\bar{M}_v = 4 \times 10^6$, 1.8 g; $\bar{M}_v$ is the viscosity-average molecular weight), JH-2 ($\bar{M}_v = 2 \times 10^6$, 3.9 g), and Y ($\bar{M}_v = 7 \times 10^5$, 4.4 g), kindly furnished by Professor Yu, were fractionated by repeating fractional precipitation with carbon tetrachloride (CCl_4) as a solvent and methanol as a precipitant. The procedure was essentially the same as that reported by Rubingh and Yu.[6] Thus, methanol was added slowly to a CCl_4 solution of a PHIC sample (2×10^{-4} to 5×10^{-4} g/cm^3 in concentration) until it became turbid. The turbid solution was warmed and kept at about 40 °C. After the turbidity had disappeared, the solution was cooled to 25 °C and allowed to stand for 1–5 days until it separated completely into two phases. In this way, 34 fractions were extracted from the three samples. Fractions having nearly identical intrinsic viscosities (in tetrahydrofuran at 25 °C) were then combined and subjected to a further fractionation. This procedure was repeated four to five times, and from about 60 products so obtained, 19 appropriate fractions were selected. Each of these 19 fractions was further divided into three parts, and the middle parts designated below as F-1, F-2, ..., F-19 were chosen for the present study. These final fractions were reprecipitated from CCl_4 solutions into methanol, freeze-dried from benzene solutions, dried overnight in vacuo at room temperature, and stored at −20 °C until use.

Hexene was fractionally distilled, with calcium hydride added.

Light Scattering. Intensities of light scattered from PHIC in hexane at 25 °C were measured on a Fica automatic light-scattering photometer in an angular range from 15 to 150°. Vertically polarized incident light of 436-nm wavelength was used for lower-molecular-weight fractions (F-1 to F-7) and that of 546 nm for higher-molecular-weight fractions (F-8 to F-19). Rayleigh's ratios for benzene of 25 °C at 436 and 546 nm were taken to be 46.5×10^{-6} and 16.1×10^{-6} cm^{-1}, respectively.[7] The depolarization ratio ρ_u of benzene determined by the method of Rubingh and Yu[6] was 0.40 at both 436 and 546 nm. The two highest-molecular-weight fractions were also examined at scattering angles between 8 and 41° (for F-18) and between 8 and 20° (for F-19) by using a He–Ne laser light-scattering photogoniometer.[8] The experimental procedures were the same as those described elsewhere.[8] Rayleigh's ratio for benzene of 25 °C for vertically polarized incident light of 632.8 nm was assumed to be 11.84×10^{-6} cm^{-1}.[9]

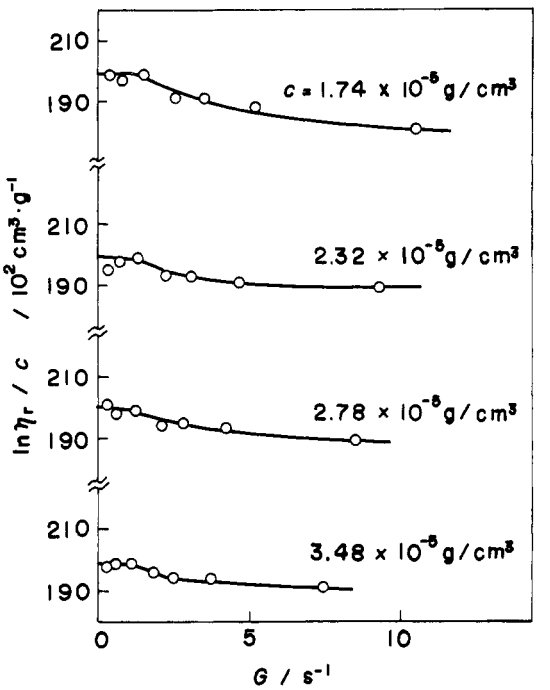

Figure 1. Dependence of $(\ln \eta_r)/c$ on shear rate G for PHIC fraction F-19 in hexane at 25 °C.

Polymer solution and the solvent hexane were made optically clean by centrifugation at 4×10^4 to 2×10^4 gravities for 2.5 to 3.5 h in a Sorvall Type RC2-B centrifuge. Each of them was transferred directly into the light-scattering cell with a carefully cleaned pipet.

The optical anisotropy of fractions F-1, F-6, F-8, F-9, and F-11 in hexane at 25 °C was investigated, with the polarizer oriented in the vertical direction. When the light-scattering envelopes observed with the analyzer set in the vertical direction and without the analyzer were compared, no difference was detected for any of these fractions. Furthermore, the scattered intensity of the lowest-molecular-weight fraction F-1 measured with the analyzer set in the horizontal direction was no more than 0.5% of the intensity measured with no analyzer, at every angle studied. These results suggest that the optical anisotropy of the PHIC molecule is negligible in the range of molecular weight studied. Hence, no anisotropy correction was applied to any of the light-scattering data obtained in this work.

The specific refractive index increments for PHIC in hexane at 25 °C were 0.134 cm^3/g at 436 nm and 0.129 cm^3/g at 546 nm. The value at 632.8 nm was estimated by linear extrapolation of these values plotted against λ^{-2}, where λ denotes the wavelength.

Viscometry. Viscosities of four PHIC fractions F-1, F-2, F-3, and F-4 in hexane at 25 °C were measured in a capillary viscometer of the Ubbelohde suspended-level type. The flow time for the solvent was about 280 s, so that no correction for kinetic energy was needed. For all other fractions, a rotational viscometer[10] of the Zimm–Crothers type was used. Figure 1 illustrates the shear-rate dependence of $(\ln \eta_r)/c$ for the highest-molecular-weight fraction F-19, where η_r and c denote, respectively, the relative viscosity and the polymer mass concentration. For any c indicated, the values of $(\ln \eta_r)/c$ at shear rates G lower than 1.5 s^{-1} are almost independent of G and may be equated to the zero-shear value. On the basis of this finding, the measurement in the rotational viscometer was made at a fixed rotor speed for which the condition $G < 1.5$ s^{-1} was satisfied.

Ultracentrifugation. 1. Sedimentation Equilibrium. To check the values of $\bar{M}_w$ (the weight-average molecular weight) from light scattering, sedimentation equilibrium measurements were made on fractions F-1, F-4, F-6, and F-8 in a Spinco Model E ultracentrifuge, with hexane of 25 °C as the solvent. A Kel-F 12-mm double-sector cell was used and the length of the liquid

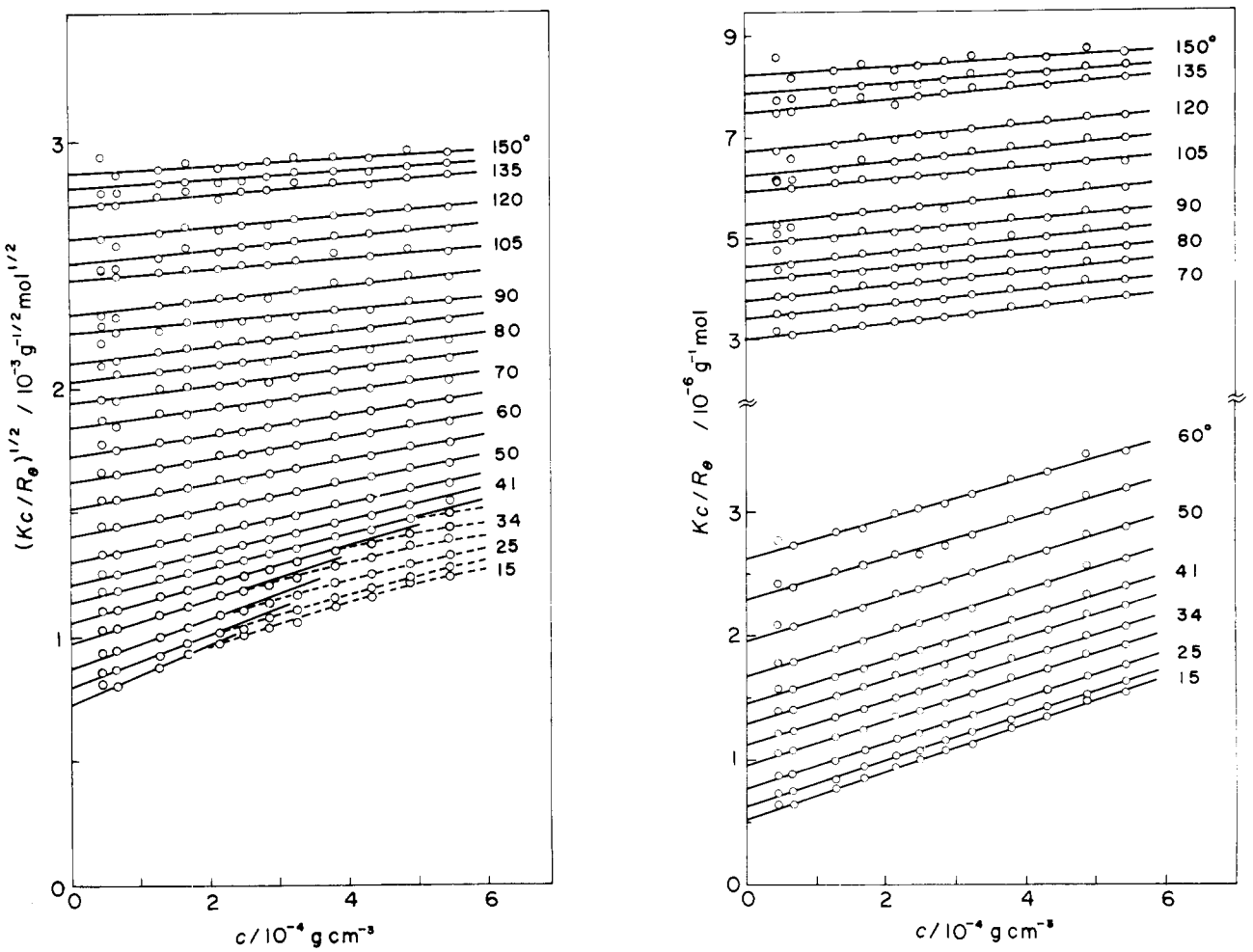

Figure 2. Plots of Kc/R_θ and $(Kc/R_\theta)^{1/2}$ against c for PHIC fraction F-15 in hexane at 25 °C.

column was adjusted to 1.5–2.5 mm. The rotor speeds in rpm were 6800 for F-1, 5200 for F-4, 4800 for F-6, and 4000 for F-8. Rayleigh fringe patterns photographed on Kodak spectroscopic plates were read on a Nikon Shadowgraph Model 6. The partial specific volume of PHIC in hexane at 25 °C was found to be 0.950 cm^3/g.

From the sedimentation equilibrium data so obtained the ratios of $\bar{M}_z$ (the z-averagae molecular weight) to $\bar{M}_w$ were estimated in the manner described elsewhere.[11] The accuracy of the estimated ratios was only moderate, being from ±10 to ±15%.

2. Sedimentation Velocity. Sedimentation velocities of PHIC in hexane at 25 °C were measured at a rotor speed of 48000 rpm with the use of a Kel-F 30-mm single-sector cell. Sedimentation coefficients s were evaluated from the slopes of ln r_p plotted against time t of centrifugation, where r_p is the radial distance from the center of rotation to the peak position in the schieren pattern. For fractions F-12, F-13, and F-19, the data were also taken at several rotor speeds between 28000 and 44000 rpm, with the result that no dependence of s on the rotor speed was detected. On the basis of this finding together with the fact that the plots of ln r_p vs. t were linear, the pressure dependence of s of PHIC in hexane was assumed negligble.

Results

Light Scattering. In Figure 2, the values of Kc/R_θ and $(Kc/R_\theta)^{1/2}$ for fraction F-15 in hexane at 25 °C are plotted against c, in order to see which of the two plots is more linear. Here R_θ is the reduced scattered intensity at a scattering angle θ and K is an optical constant. The Kc/R_θ vs. c plot is linear at every θ indicated whereas the square-root plots at θ lower than 34° show an appreciable downward curvature. Since similar results were obtained for all other fractions, the Kc/R_θ vs. c plot was adopted for analysis of the concentration dependence of scattered intensities. For the angular dependence, Berry's square-root plot,[12] i.e., $(Kc/R_\theta)^{1/2}$ vs. $\sin^2\theta/2$, was used. In Figure

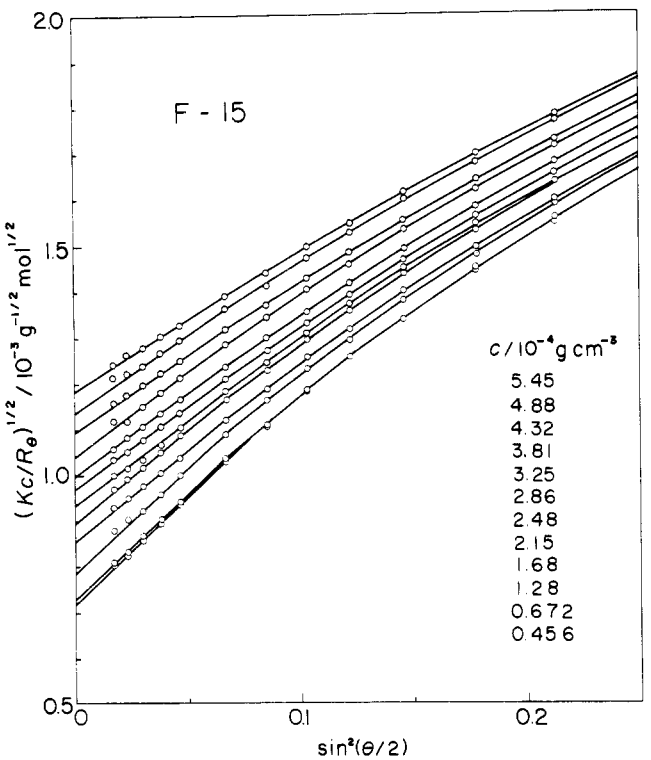

Figure 3. Plots of $(Kc/R_\theta)^{1/2}$ vs. $\sin^2(\theta/2)$ for PHIC fraction F-15 in hexane at 25 °C.

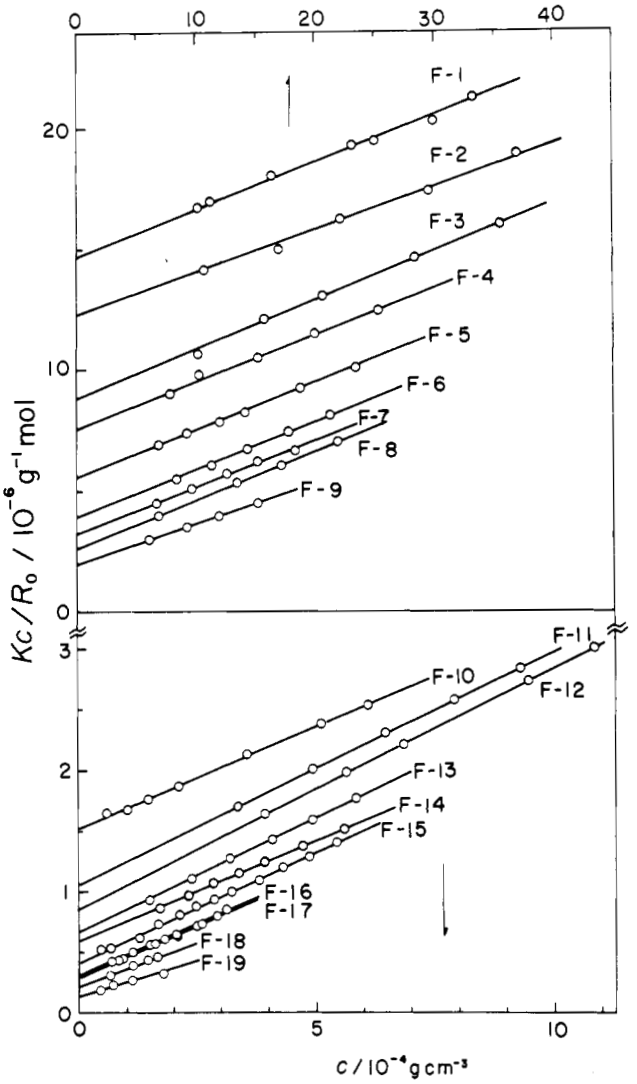

Figure 4. Plots of $(Kc/R_\theta)_{\theta=0}$ vs. c for all PHIC fractions studied.

Table I
Numerical Results from Light Scattering and Sedimentation Equilibrium Measurements on PHIC Fractions in Hexane at 25 °C

fraction	$\bar{M}_w \times 10^{-4}$	$A_2 \times 10^4$ [a]	$\langle S^2\rangle_z \times 10^{10}$, cm^2	$\bar{M}_z/\bar{M}_w$
F-1	6.80	9.8	(0.0515)	
	6.80[b]	9.8[b]		1.0$_5$[b]
F-2	8.14	8.8	0.0686	
F-3	11.2	9.9	0.107	
F-4	13.2	9.6	0.144	
	12.8[b]	10.2[b]		1.0$_5$[b]
F-5	18.0	9.8	0.223	
F-6	25.5	9.8	0.352	
	24.4[b]	9.9[b]		1.0$_5$[b]
F-7	31.1	9.7	0.467	
F-8	38.7	10.1	0.603	
	39.2[b]	11.2[b]		1.0$_5$[b]
F-9	50.5	8.3	0.836	
F-10	65.6	8.3	1.13	
F-11	94.7	9.5	1.65	
F-12	117	9.9	2.08	
F-13	149	9.3	2.67	
F-14	169	8.2	3.13	
F-15	241	8.9	4.63	
F-16	318	8.1	6.29	
F-17	334	8.4	6.67	
F-18	463	7.5	10.0	
F-19	724	5.4	17.4	

[a] In units of cm^3 mol/g^2. [b] From sedimentation equilibrium.

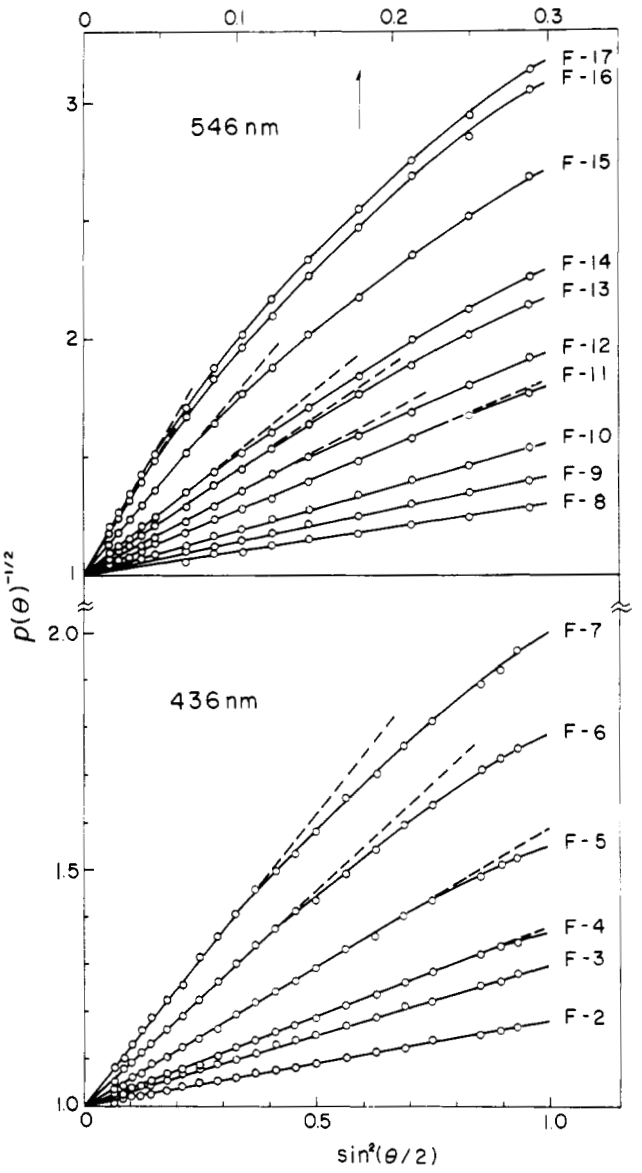

Figure 5. Angular dependence of $P(\theta)^{-1/2}$ for the indicated PHIC fractions.

3, the advantage of this type of plot is illustrated with the data for fraction F-15.

Figure 4 shows plots of $(Kc/R_\theta)_{\theta=0}$ vs. c for all the PHIC fractions studied. The values of $\bar{M}_w$ and A_2 (the second virial coefficient) evaluated from the indicated straight lines are summarized in Table I, together with the values of $\bar{M}_w$, A_2, and $\bar{M}_z/\bar{M}_w$ determined by sedimentation equilibrium. The $\bar{M}_w$ values from the two different methods agree within experimental error. The ratios of $\bar{M}_z$ to $\bar{M}_w$ indicate that fractions F-1, F-4, F-6, and F-8 are narrow in molecular weight dispersion. In Figures 5 and 6 the plots of $P(\theta)^{-1/2}$ vs. $\sin^2(\theta/2)$ for all the fractions (except for F-1) are illustrated, where $P(\theta)$ denotes the particle scattering function. In the latter figure, the data from the Fica light-scattering photometer and the laser light-scattering photometer are compared. The values of $\langle S^2\rangle_z$ evaluated from the dashed lines in Figures 5 and 6 are listed in the fourth column of Table I. The value of $\langle S^2\rangle_z$ for fraction F-1 in this table is not very accurate because the slope of the $P(\theta)^{-1/2}$ vs. $\sin^2(\theta/2)$ line was not large enough for an accurate determination. The molecular weight dependence of the characteristic ratio $\langle S^2\rangle_z/\bar{M}_w$ is depicted in Figure 7, together with the data reported by Rubingh and Yu.[6] With the increase in $\bar{M}_w$, the charac-

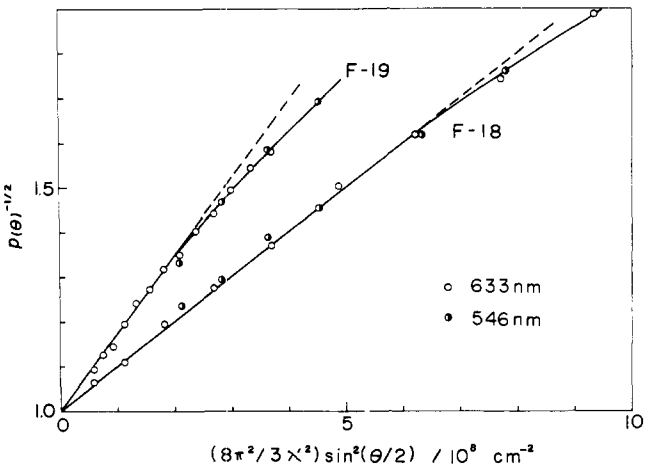

Figure 6. Angular dependence of $P(\theta)^{-1/2}$ for PHIC fractions F-18 and F-19, where λ' denotes the wavelength of incident light in solution: (○) laser light-scattering photometer and (◑) Fica light-scattering photometer.

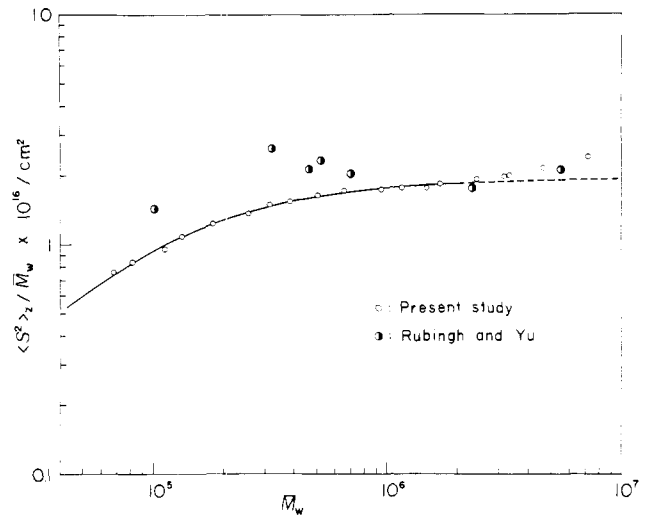

Figure 7. Molecular weight dependence of the characteristic ratio $\langle S^2\rangle_z/\bar{M}_w$ for PHIC in hexane at 25 °C: (○) this work and (◑) Rubingh and Yu.[6]

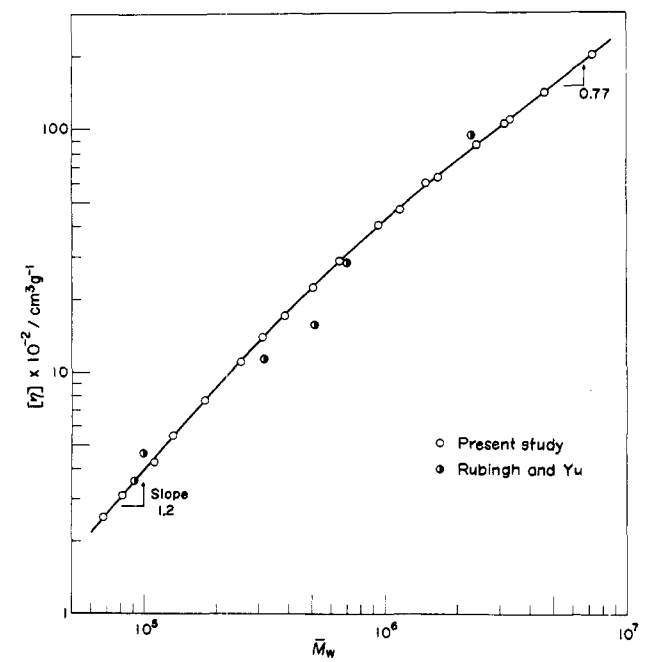

Figure 8. Double-logarithmic plots of $[\eta]$ vs. $\bar{M}_w$ for PHIC in hexane at 25 °C: (○) this work and (◑) Rubingh and Yu.[6]

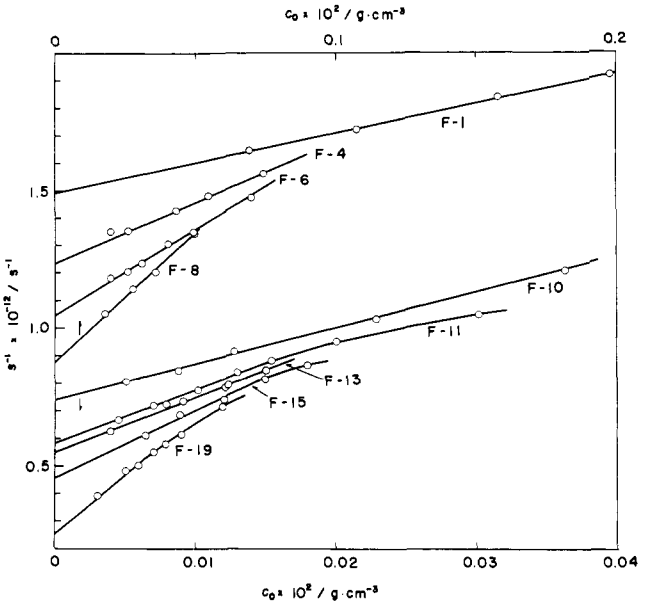

Figure 9. Concentration dependence of s^{-1} for the indicated PHIC fractions in hexane at 25 °C.

Table II
Numerical Results from Viscosity and Sedimentation Velocity Measurements on PHIC Fractions in Hexane at 25 °C

fraction	$[\eta] \times 10^{-2}$, cm^3 g^{-1}	k'	$s_0 \times 10^{13}$, s	$k_s \times 10^{-2}$, cm^3 g^{-1}
F-1	2.51	0.39	6.71	1.47
F-2	3.10	0.38	7.34	1.94
F-3	4.26	0.39	7.87	3.50
F-4	5.50	0.38	8.10	3.52
F-5	7.70	0.39	8.81	4.42
F-6	11.1	0.38	9.57	5.77
F-7	14.0	0.38	10.2	7.28
F-8	17.2	0.37	11.4	10.4
F-9	22.5	0.38	13.1	16.3
F-10	29.0	0.38	13.5	17.6
F-11	40.4	0.43	17.1	32.3
F-12	47.0	0.38	18.0	36.0
F-13	60.4	0.42	18.2	35.9
F-14	63.6	0.41	20.0	45.2
F-15	86.0	0.42	22.0	52.3
F-16	105	0.41	25.3	72.2
F-17	109	0.39	26.0	81
F-18	141	0.49	30.8	101
F-19	200	0.50	36.4	143

teristic ratio first increases monotonically and then appears to level off at a constant value. This behavior is consistent with the known fact that PHIC is a stiff polymer.

Intrinsic Viscosity and Sedimentation Coefficient. The values of $[\eta]$ and k' (Huggins' constant) for all 19 fractions of PHIC in hexane at 25 °C are summarized in Table II, and the $[\eta]$ values are plotted double-logarithmically against $\bar{M}_w$ in Figure 8. The plotted points are fitted by a smooth curve convex upward. The slope of the curve is about 1.2 for $\bar{M}_w$ between 7×10^4 and 4×10^5 and about 0.77 for $\bar{M}_w$ higher than 10^6. This change in slope suggests that the PHIC molecule is rodlike in the lower-molecular-weight range and approaches a spherical random coil as $\bar{M}_w$ increases.

Figure 9 illustrates plots of s^{-1} vs. initial polymer concentration c_0 for the indicated PHIC fractions in hexane at 25 °C. The values of s_0 and k_s (as defined by the equation $s^{-1} = s_0^{-1} + s_0^{-1}k_s c_0$) obtained from these plots are given in Table II. The s_0 values are plotted double-logarithmically against $\bar{M}_w$ in Figure 10. The weak dependence of s_0 on $\bar{M}_w$ (the slope is 0.26 for $7 \times 10^4 < \bar{M}_w <$

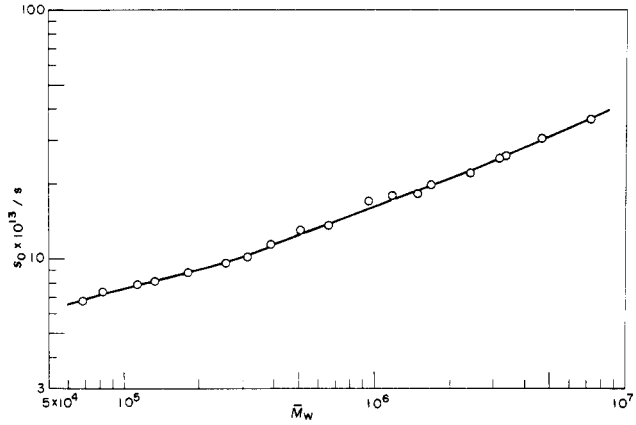

Figure 10. Double-logarithmic plots of s_0 vs. $\bar{M}_w$ for PHIC in hexane at 25 °C.

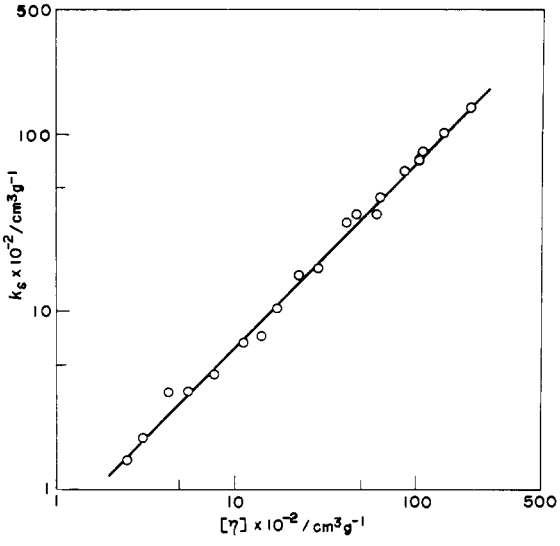

Figure 11. Relation between k_s and $[\eta]$ for PHIC in hexane at 25 °C.

3×10^5) is another evidence for the semiflexibility of the PHIC chain. The relation between k_s and $[\eta]$, shown in Figure 11, has a slope of 1.04, indicating that a close correlation exists between k_s and $[\eta]$ for PHIC.

Discussion

Molecular Dimensions and Particle Scattering Function. 1. Determination of the Wormlike Chain Parameters. According to Benoit and Doty,[13] the unperturbed $\langle S^2 \rangle$ of a monodisperse wormlike chain is expressed by

$$\langle S^2 \rangle = (qM/3M_L) - q^2 + (2q^3M_L/M)[1 - (qM_L/M)(1 - e^{-M/qM_L})] \quad (1)$$

with the molecular weight M, the persistance length q, and the shift factor M_L. Equation 1 can be approximated by

$$(M/\langle S^2 \rangle)^{1/2} = (3M_L/q)^{1/2}(1 + 3qM_L/2M) \quad (2)$$

the maximum deivation from the exact value being 0.5% for $M/2qM_L > 4$ and 1% for $M/2qM_L > 2$. Thus, if $M/2qM_L > 2$, the values of $(M/\langle S^2 \rangle)^{1/2}$ plotted against M^{-1} should give a straight line whose intercept and slope are equal to $(3M_L/q)^{1/2}$ and $3M_L(3qM_L)^{1/2}/2$, respectively, and allow the two parameters q and M_L to be evaluated.

If this method is applied to our $\langle S^2 \rangle_z$ data for PHIC, the result as shown in Figure 12 is obtained. Except for the four points at small $\bar{M}_w^{-1}$, the data points follow a straight line, as is expected from eq 2. The values of q and M_L determined from this line are given in Table III, together

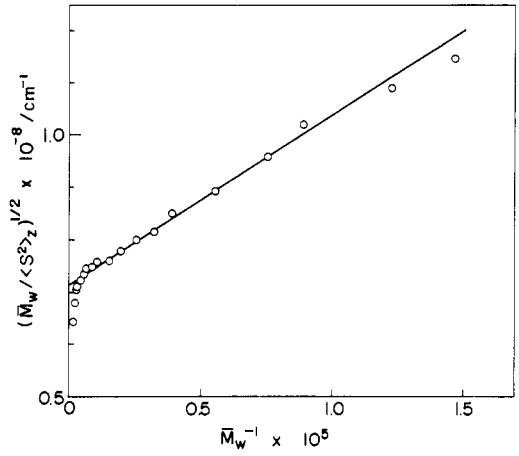

Figure 12. Plots of $(\bar{M}_w/\langle S^2 \rangle_z)^{1/2}$ vs. $\bar{M}_w$ for PHIC in hexane.

Table III
Wormlike Chain Parameters of Poly(hexyl isocyanate)

source	q, nm	M_L, nm^{-1}	solvent
this work	42 ± 1	715 ± 15	hexane of 25 °C
Rubingh and Yu[6]	42 ± 2	640 ± 70	hexane of 25 °C
Berger and Tidswell[5]	42.5	640 (assumed)	tetrahydrofuran of 25 °C

with the values estimated from $\langle S^2 \rangle_z$ by Rubingh and Yu[6] and by Berger and Tidswell,[5] using a curve-fitting method. The q values obtained by the three groups are in almost complete agreement. However, it is to be noted that Berger–Tidswell's q value was derived on the assumption that M_L equals 640 nm^{-1}. The agreement between Rubingh–Yu's and our M_L values is not as good as that with respect to q. Our M_L value 715 ± 15 nm^{-1} yields 0.178 ± 0.003 nm for the contour length per monomer; this value happens to coincide with the helix pitch (per monomer) of 0.18 nm deduced by Troxell and Scheraga[14] from a conformational calculation of the poly(methyl isocyanate) chain. Although the correlation between the local structure of a real polymer chain and the parameter M_L of the wormlike chain is not clear, this agreement implies that the Troxell–Scheraga helix (eight monomers in three turns) describes the local conformation of poly(alkyl isocyanates) in dilute solution.

2. Comparison between Theory and Experiment. Figure 13 compares our data of $\langle S^2 \rangle_z$ for PHIC with the theoretical values (the solid line) computed from eq 1 with q = 42 nm and M_L = 715 nm^{-1}; the solid line in Figure 7 also represents the same theoretical values. These figures indicate that the wormlike chain model describes accurately the chain length dependence of the dimensions of the PHIC chain in hexane. The deviation of the four data points at $\bar{M}_w$ above 3×10^6 from the solid lines may be ascribed to the excluded-volume effect. The linear expansion factor as calculated from the measured $\langle S^2 \rangle_z$ divided by the theoretical value is 1.11 for the highest-molecular-weight fraction.

In Figure 14, our data of the $P(\theta)$ function for PHIC are compared with the values calculated from either the Sharp–Bloomfield theory[15] or the numerical table given by Yamakawa and Fujii,[16] using the indicated values of q and M_L. Here comparison is restricted to fractions exhibiting the unperturbed wormlike chain behavior. Since these values of q and M_L are within the bounds of the corresponding values estimated from $\langle S^2 \rangle_z$ (see Table III) and also since the indicated $\bar{M}_z/\bar{M}_w$ values suggest that our PHIC fractions are quite narrow in molecular weight distribution, it can be concluded that PHIC in hexane is

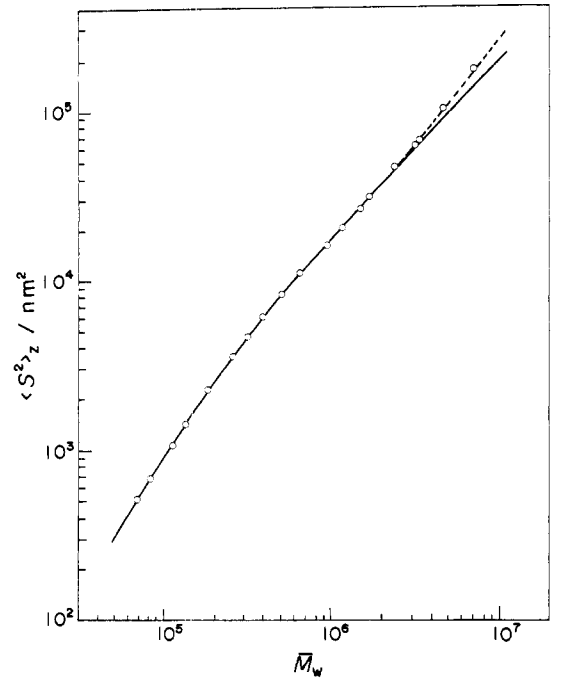

Figure 13. Comparison of the measured $\langle S^2 \rangle_z$ with the theoretical values (solid line) calculated from eq 1 with q = 42 nm and M_L = 715 nm^{-1}.

an excellent model polymer for the wormlike chain, sufficiently entitled to be used for checking Yamakawa–Fujii's hydrodynamic theories[1,2] for the wormlike cylinder.

Comparison of Data for $[\eta]$ and s_0 with Yamakawa–Fujii's Theories. In Yamakawa–Fujii's theories,[1,2] both $[\eta]$ and s_0 of a wormlike cylinder are expressed as functions of q, M_L, and an additional hydrodynamic parameter d, the diameter of the cylinder. A d value fitting our experimental curve of log $[\eta]$ vs. log $\bar{M}_w$ to Yamakawa–Fujii's theoretical one was sought by trial and error, with q and M_L fixed, respectively, to 42 and 715 nm^{-1}, and it was found that the values 1.6 ± 0.2 nm lead to the most satisfactory agreement. In Figure 15, the solid line corresponding to q = 42 nm, M_L = 715 nm^{-1}, and d = 1.6 nm is seen to agree closely with the measured values. This d value is consistent with the value of 1.3 nm that can be estimated for the helix diameter of poly(butyl isocyanate) from crystallographic data.[17] The fact that the theory fits the data points even for $\bar{M}_w$ above 3×10^6 implies that the excluded-volume effect on $[\eta]$ is not as large as that on $\langle S^2 \rangle_z$. What is more important is the fact that the d value consistent with the $[\eta]$ data does not bring Yamakawa–Fujii's theoretical equation for s_0 to a close fit to our experimental points; the appreciable deviation occurs at $\bar{M}_w$ below 7×10^5. A better agreement as illustrated by a dashed line is obtained if d is increased to about 2.5 nm. However, this d leads to a poor agreement between the experimental and theoretical values of $[\eta]$ (see the dashed line for $[\eta]$). A similar discrepancy was encountered in a recent study on DNA by Godfrey and Eisenberg,[3] who found that the d value (2.6 nm) derived from s_0 data was about twice that from $[\eta]$ (1.2 nm). This d value from s_0 is in agreement with the diameter of a double-stranded DNA estimated from X-ray diffraction and scattering.[18] Hence the value of 1.2 nm from $[\eta]$ is considered too small for the DNA. On the other hand, the d value of 1.6 nm for PHIC from $[\eta]$ is reasonable, while the value of 2.5 nm from s_0 is too large when estimated from the chemical structure of the PHIC repeat unit, which suggests that the chain diameter be in a range between 1.2 and 1.8 nm.

For a more critical comparison of our s_0 values with Yamakawa–Fujii's theory, they are plotted against $\bar{M}_w^{1/2}$ in Figure 16, where the solid and dot-dash lines represent the theoretical values calculated, respectively, for d = 2.5 nm and 1.6 nm, with q and M_L fixed for both cases. The data points are consistent with the solid line over the entire range of $\bar{M}_w$. The linear region may be fitted to the asymptotic equation derived from Yamakawa–Fujii's theory, i.e.,

$$s_0 = [(1 - \bar{v}\rho_0)/(3\pi\eta_0 N_A)] \times [1.843(M_L/2q)^{1/2}M^{1/2} + M_L f(d/2q)] \quad (3)$$

where $\bar{v}$ is the partial specific volume of the polymer, ρ_0 and η_0 are, respectively, the density and viscosity of the solvent, N_A is Avogadro's constant, and $f(d/2q)$ is a known function of $d/2q$. The dashed line calculated from eq 3,

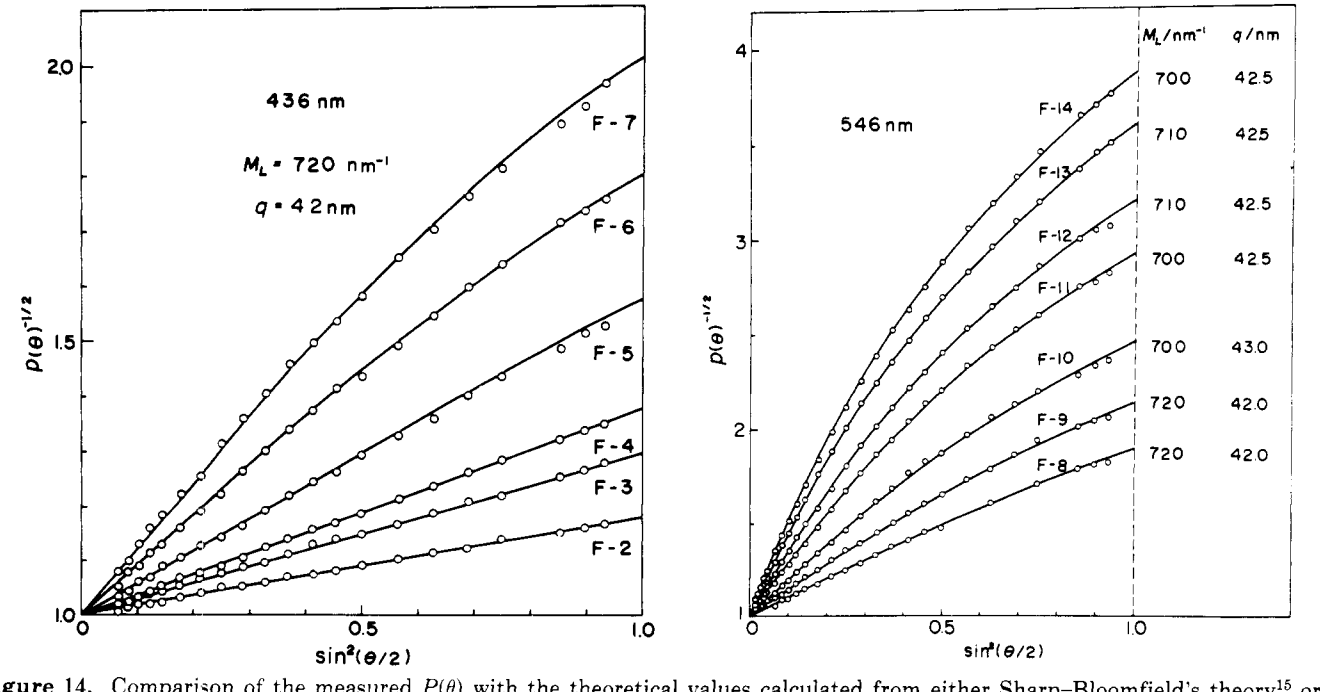

Figure 14. Comparison of the measured $P(\theta)$ with the theoretical values calculated from either Sharp–Bloomfield's theory[15] or Yamakawa–Fujii's numerical table,[16] using the indicated values of q and M_L.

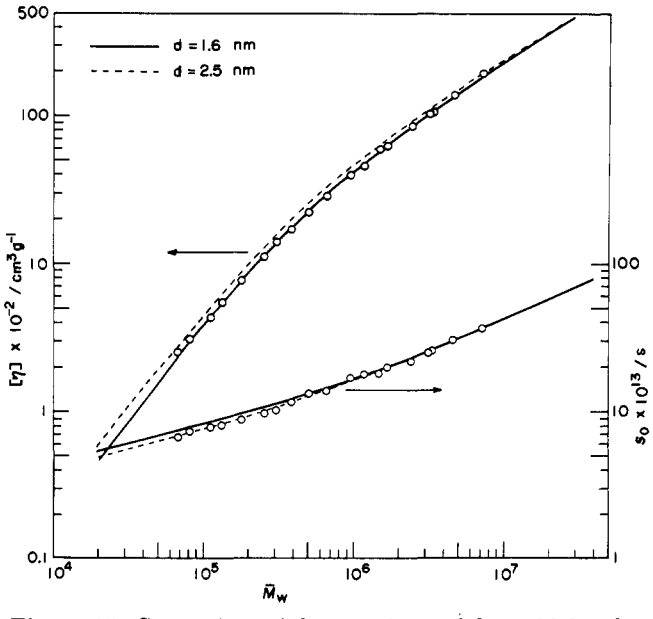

Figure 15. Comparison of the experimental data of $[\eta]$ and s_0 with Yamakawa–Fujii's theories; the solid and dashed lines are calculated, respectively, for d = 1.6 and 2.5 nm with both q and M_L fixed to the same values as those used for Figure 13.

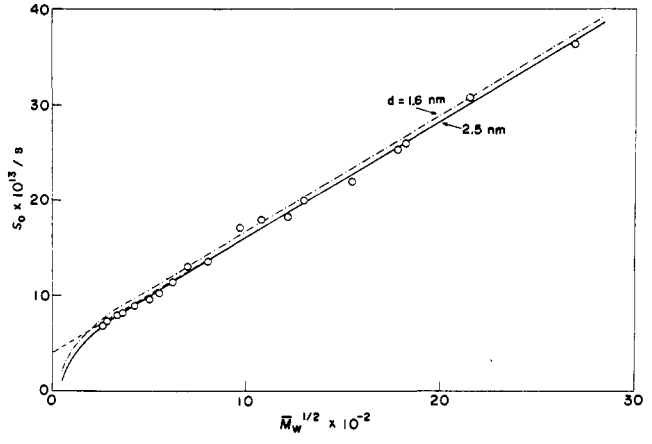

Figure 16. Plots of s_0 vs. $\bar{M}_w^{1/2}$ for PHIC in hexane. The solid and dot-dash lines indicate Yamakawa–Fujii's theoretical values for d = 2.5 and 1.6 nm, respectively; the values of q and M_L are the same as those used for Figure 13. The dashed line is calculated from eq 3 with the same parameter values as those used for the solid line.

using the same parameter values as for the solid line, is indistinguishable from the solid line down to $\bar{M}_w^{1/2} \sim 6 \times 10^2$. Furthermore, the dot-dash line is accurately parallel to these lines for $\bar{M}_w^{1/2}$ above 5×10^2. From these features of the calculated curves and the experimental points, we find that since the slope of the experimental s_0 vs. $\bar{M}_w^{1/2}$ plot for $\bar{M}_w^{1/2}$ above 6×10^2 is consistent with q = 42 nm and M_L = 715 nm^{-1} and not affected by d, the leading term in eq 3 describes correctly the molecular weight dependence of the measured s_0 and the function $f(d/2q)$ in the second term is the source of our seemingly unreasonable d value of 2.5 nm.

Figure 17 shows the molecular weight dependence of Flory's viscosity factor Φ defined by

$$[\eta] = \Phi(6\langle S^2\rangle_z)^{3/2}/\bar{M}_w \qquad (4)$$

The solid line represents the theoretical values calculated from Benoit–Doty's theory[13] for $\langle S^2\rangle$ and Yamakawa–Fujii's theory[2] for $[\eta]$ with q = 42 nm, M_L = 715 nm^{-1}, and d = 1.6 nm. An interesting feature is that both the experimental and theoretical curves exhibit a shallow minimum at about an $\bar{M}_w$ value of 1.7×10^5. The deviation of the data points from the theoretical curve at $\bar{M}_w$ above 3×10^6 may be ascribed to the excluded-volume effect on $\langle S^2\rangle_z$. It should be noted that the maximum Φ value obtained is still about one-half the theoretical value 2.87×10^{23} mol^{-1} for infinitely long, flexible chains.[2,19]

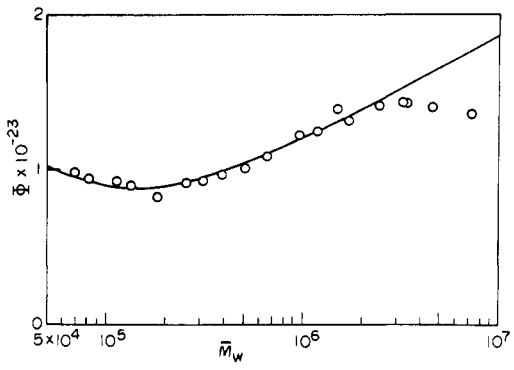

Figure 17. Molecular-weight dependence of Flory's viscosity factor Φ (in mol^{-1}) for PHIC in hexane. The solid line indicates the theoretical values calculated from Yamakawa–Fujii's theory and eq 1 with q = 42 nm, M_L = 715 nm^{-1}, and d = 1.6 nm.

In conclusion, the dimensions and the particle scattering function of PHIC in hexane are described accurately by the wormlike chain model, but Yamakawa–Fujii's theories for $[\eta]$ and s_0 of the wormlike cylinder model cannot be fitted to the experimental data unless inconsistent diameter values are used for $[\eta]$ and s_0. The point to note is that the diameter value fitting our s_0 data is seemingly incompatible with the chemical structure of the PHIC repeat unit, differing from Godfrey–Eisenberg's work[3] on DNA, in which a very reasonable diameter value was obtained from s_0. In any event, our experimental results on PHIC as well as Godfrey–Eisenberg's on DNA suggest that the physical approximations basic to Yamakawa–Fujii's hydrodynamic theories for the wormlike cylinder be subjected to a careful reexamination.

Acknowledgment. We are grateful to Professor H. Yu at the University of Wisconsin for the gift of the PHIC samples and for his interest in the present study.

References and Notes

(1) H. Yamakawa and M. Fujii, *Macromolecules*, **6**, 407 (1973).
(2) H. Yamakawa and M. Fujii, *Macromolecules*, **7**, 128 (1974).
(3) J. E. Godfrey and H. Eisenberg, *Biophys. Chem.*, **5**, 301 (1976).
(4) N. S. Schneider, S. Furusaki, and R. W. Lenz, *J. Polym. Sci., Part A*, **3**, 933 (1965).
(5) M. N. Berger and B. M. Tidswell, *J. Polym. Sci., Part C*, **No. 42**, 1063 (1973).
(6) D. N. Rubingh and H. Yu, *Macromolecules*, **9**, 681 (1976).
(7) Gj. Deželić and J. Vavra, *Croat. Chem. Acta*, **38**, 35 (1966).
(8) Y. Einaga, T. Mitani, J. Hashizume, and H. Fujita, *Polym. J.*, **11**, 565 (1979).
(9) E. R. Pike, W. R. M. Pomeroy, and J. M. Vaughan, *J. Chem. Phys.*, **62**, 3188 (1975).
(10) Y. Einaga, Y. Miyaki, and H. Fujita, *J. Soc. Rheol. Jpn.*, **5**, 188 (1977).
(11) T. Norisuye, T. Yanaki, and H. Fujita, *J. Polym. Sci., Polym. Phys. Ed.*, in press.
(12) G. C. Berry, *J. Chem. Phys.*, **44**, 4550 (1966).
(13) H. Benoit and P. Doty, *J. Phys. Chem.*, **57**, 958 (1953).
(14) T. C. Troxell and H. A. Scheraga, *Macromolecules*, **4**, 528 (1971).
(15) P. Sharp and V. A. Bloomfield, *Biopolymers*, **6**, 1201 (1968).
(16) H. Yamakawa and M. Fujii, *Macromolecules*, **7**, 649 (1974).
(17) U. Shmueli, W. Traub, and K. Rosenheck, *J. Polym. Sci., Part A-2*, **7**, 515 (1969).
(18) V. A. Bloomfield, D. M. Crothers, and I. Tinoco, "Physical Chemistry of Nucleic Acids", Harper and Row, New York, 1974, Chapter 5.
(19) P. L. Auer and C. S. Gardner, *J. Chem. Phys.*, **23**, 1545, 1546 (1955).